RAPID COMMUNICATIONS

PHYSICAL REVIEW B VOLUME 52, NUMBER 18 1 NOVEMBER 1995-II

Reversible propagating fingers in an antiferroelectric liquid crystal

Jian-feng Li, Xin-Yi Wang, Erik Kangas,* P. L. Taylor, and Charles Rosenblatt†
Department of Physics, Case Western Reserve University, Cleveland, Ohio 44106

Yoshi-ichi Suzuki
Central R&D Laboratory, Showa Shell Sekiyu Kabushiki Kaishi, Kanagawa-ken, Japan

P. E. Cladis
AT&T Bell Laboratories, Murray Hill, New Jersey 07974
(Received 28 August 1995)

Propagating fingerlike solitary waves are observed in an antiferroelectric liquid crystal on application of an electric field above a threshold field E_{th}. On reducing the field below E_{th} the fingers recede, also as solitary waves. The velocity of the waves, which to our knowledge is the fastest observed for a liquid crystal, scales approximately as $E-E_{th}$ for E near E_{th}. A simple model, which includes a layer-layer coupling term, is presented and describes much of the observed behavior.

The physics of liquid crystals is rich and varied, with over three dozen phases currently known. In recent years some of the most exciting results, both scientific and technological, have come from the antiferroelectric liquid crystalline (AFLC) phase,[1-3] which exhibits three states in a polarization (P)-electric field (E) hysteresis loop. AFLCs have a layered (smectic) structure in which molecules, typically about 30 Å long and about 5 Å in diameter, are tilted in one layer by an angle θ relative to the layer normal and by $-\theta$ in the two neighboring layers, with anisotropic fluidity within the layer plane (see Fig. 1). For each smectic layer there is a polarization P_0 which lies in the plane of the layer and perpendicular to the molecules, such that in adjacent layers the polarization vectors are nearly antiparallel. Thus in zero field the net polarization vanishes. In bulk samples, molecules in the odd layers (for example) and those in the even layers form a pair of long-pitch helical structures along an axis normal to the layers, where the pitch is typically of the order of thousands of angstroms to several microns. In a sufficiently large applied electric field the helices unwind, giving rise to field-induced long-range ferroelectric ordering[4] characterized by a saturated net polarization and a molecular tilt θ relative to the layer normal. Ferrielectric states, which in our system are defined such that adjacent layers are characterized by polarizations which are no longer opposite, connect the $P=0$ antiferroelectric state to the fully saturated polarization of the ferroelectric state.

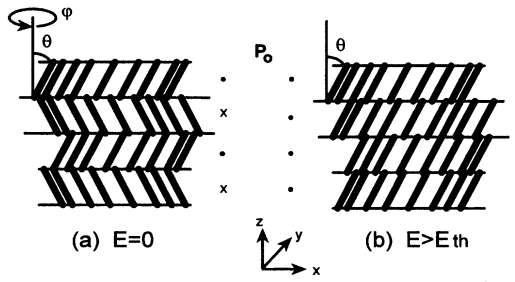

FIG. 1. Schematic representation of (a) surface stabilized antiferroelectric state, and (b) field driven ferroelectric state. The magnitude of the polar tilt angle is θ and the azimuthal orientation is φ. In the presence of an electric field $E>E_{th}$ the azimuthal orientation φ_{i+1} of the odd layer remains unchanged, but that of the even layers φ_i rotates into alignment with the field, as shown in b. The local polarization P_0 in alternating layers is shown.

In AFLCs it has been observed that the transition from the highest-field ferrielectric state to a ferroelectric state is characterized by ferroelectric fingers invading the ferrielectric region,[5] even at frequencies of 1 kHz. While it was suggested that the dynamics of this transition at a driving frequency of $f=1$ kHz is propagative (rather than diffusive), no quantitative data was presented, and there appears to be little previous theoretical analysis of this problem. Here we show quantitatively that the AFLC ferrielectric-ferroelectric transition at $f=0$ is characterized by a threshold field E_{th} that is independent of sample thickness. Moreover, we show that the propagation speed $v=v_0(E-E_{th})/E_{th}$ for $|(E-E_{th})/E_{th}|\ll 1$, with v_0 a material-dependent speed that is typically a few centimeters per second. Finally, we observe that the fingering is reversible when E is reduced below E_{th}. We model these results with an elastic energy that includes dielectric effects and, importantly, an interlayer coupling. In this model the dynamics are driven by dielectric effects and the interlayer coupling determines E_{th}. These features account for the independence of E_{th} on sample thickness. Both the model and the experiment reveal important physics which connect the antiferroelectric and ferroelectric liquid crystal phases.

Cells were constructed of electrically conducting indium-tin-oxide coated glass plates, which were first dipped in a solution of nylon 6/6 in formic acid and allowed to drip dry. The slides were then rubbed unidirectionally, placed together (with the rubbing directions parallel) separated by a pair of

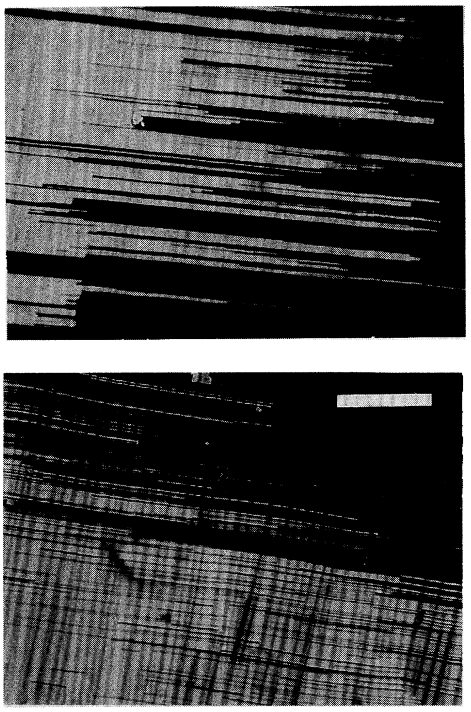

FIG. 2. Polarized photomicrographs of finger textures, both at 110 °C. (a) Nylon treated surface, and (b) polyimide treated surface. The fingering direction corresponds to the $\hat{x}$ axis, and the direction perpendicular to the fingers, but still in the plane of the image, is the $\hat{z}$ axis. The fingers were stabilized at an electric field just above E_{th}, and the polarizer and analyzer were oriented along the $\hat{y}$ and $\hat{z}$ axes, respectively (see Fig. 1). A 100-μm-long bar is shown in the lower figure.

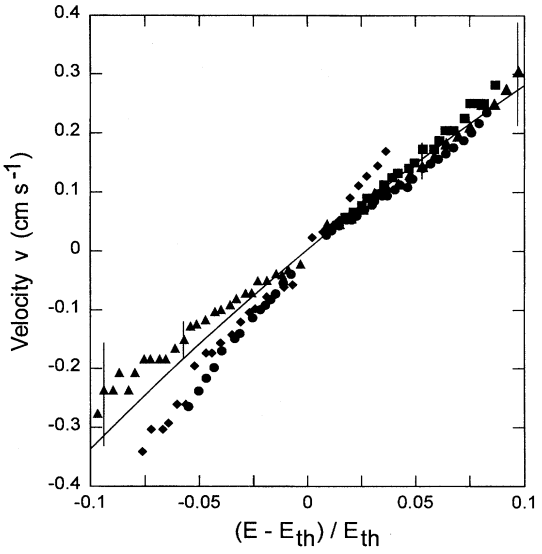

FIG. 3. Experimental velocity v of fingers vs reduced field $(E-E_{th})/E_{th}$ for nylon coated cells of thickness $d=5$ μm (▲), $d=9$ μm (■), and $d=12.5$ μm (●). Values of E_{th} are given in Table I. Data are also shown for polyimide coated cell of thickness $d=14$ μm (◆). Uncertainty in cell spacing is ± 1 μm. Several typical error bars, due primarily to the shutter speed of the CCD camera, are shown; the relative error is approximately $\pm 20\%$ at the largest reduced fields, and decreases toward $E-E_{th}/E_{th}=0$. Solid line represents model calculation [Eq. (4)] using values $P_0=225$ esu cm^{-2}, $2U=5.6\times10^4$ erg cm^{-3}, $\gamma=0.25$ poise, $\Delta\varepsilon=-1.1$, and $K=1\times10^{-6}$ dyn.

Mylar spacers of thickness d, and cemented. The cell spacings d varied from 2 to 14 μm. The cells were filled with the liquid crystal 4-(1-trifluoromethylhexyloxycarbonyl) phenyl 4′-octyloxybiphenyl-4-carboxylate (Ref. 6) in the isotropic phase, placed into a temperature controlled oven, and allowed to cool into the antiferroelectric Sm C_A^* phase. The temperature was stabilized at (110.00 ± 0.01) °C, i.e., ~3.5 °C below the smectic A-antiferroelectric smectic C_A^* transition, and the sample was viewed through a polarizing optical microscope; a texture-free, planar orientation was observed. A dc electric field was then applied to the sample. Below a threshold field E_{th} no obvious change in the appearance of the sample was observed; above E_{th} however, bright fingers began to appear under the crossed polarizers (Fig. 2). The appearance of fingers occurred at a characteristic threshold *field*, independent of d to within experimental uncertainty (Table I).

To measure v vs E a square wave of period 8 s was applied to the sample, and the image sent to a video cassette recorder from a charge coupled device (CCD) camera. The recording, with a spatial resolution of approximately 2 μm, was played back frame by frame, such that the temporal resolution was 0.0167 s. The position of the propagating tip of the finger—which moved with constant velocity and shape—was measured on the screen, thereby yielding the velocity vs E. In Fig. 3 we show v vs positive reduced field $(E-E_{th})/E_{th}$ for three different cell spacings [5 μm (▲), 9 μm (■), and 12.5 μm (●)] with nylon-treated surfaces; these correspond to advancing fingers. We also show v vs

TABLE I. Experimental solitary-wave parameters.

Spacer thickness (μm)	E_{th} (statv cm^{-1})	v_0 (cm s^{-1})
5±1 (nylon)	242±40	2.9±0.4 (advancing)
		−2.6±0.5 (retreating)
9±1 (nylon)	260±35	3.1±0.4 (advancing)
12.5±1 (nylon)	227±35	2.6±0.4 (advancing)
		−4.5±0.5 (retreating)
14±1 (polyimide)	263±35	4.5±0.5 (advancing)
		−4.3±0.5 (retreating)

negative reduced field (retreating fingers) for the 5 μm (▲) and 12.5 μm (●) cells. Values for E_{th} are given in Table I, where the uncertainty is due largely to the uncertainty in cell thickness. The effects of surface treatment are shown in Fig. 3 for a polyimide aligning agent with cell thickness $d=14$ μm (◆); both advancing and retreating fingers are shown. In this plot $v_0=(4.5\pm0.5)$ cm s^{-1}, while for most of the nylon surfaces (except for the retreating 12.5 μm cell) $v_0\sim(2.9\pm0.4)$ cm s^{-1}; we do not have an explanation for this one counterexample. As the density of fingers for the ferroelectric state appears to be larger for the nylon treated sample, we surmise that the surface wetting properties of the surface treatment influence the propagation. We also believe that the width of the propagating fingers is closely related to the pitch of the bulk antiferroelectric phase, as the pitch (or some fraction thereof) corresponds to a characteristic distance over which the azimuthal orientations are in register.

Much effort has been applied to the task of describing propagating solutions in nonlinear systems, and in liquid crystalline systems in particular.[7–17] To model the observed behavior, we start with the unwound helix limit of the free energy proposed by Wang and Taylor[7] for a fully chiral system. The free energy $F=\Sigma_i\int f_i dx$, where $f_i=f_i^{\text{elastic}}+f_i^{\text{electric}}+f_i^{\text{layer-layer}}$:

$$f_i=\tfrac{1}{2}K\sin^2\theta\left(\frac{\partial\varphi_i}{\partial x}\right)^2-P_0E\cos\varphi_i-\frac{\Delta\varepsilon\sin^2\theta}{8\pi}E^2\sin^2\varphi_i+\frac{U}{2}[\cos(\varphi_{i-1}-\varphi_i)+\cos(\varphi_i-\varphi_{i+1})]. \quad (1)$$

Here f_i is the free energy density of the i^{th} smectic layer; $K\sin^2\theta$ is the effective elastic constant associated with a change in azimuthal orientation φ along the $\hat{x}$ axis (within a smectic layer); P_0 is the local polarization; and $\Delta\varepsilon$ is the dielectric anisotropy. The coupling between layers is expressed in terms of the coupling coefficient U, which has dimensions of energy per volume, and represents a local interaction involving dipoles and possibly steric effects. It is the presence of this term that distinguishes the present model from previously extant models.

We now take the equations of motion found from Eq. (1) and introduce a viscosity γ associated with azimuthal rotations of the director. In the overdamped limit we find for $i=1,2,3,\ldots,n$:

$$\gamma\frac{\partial\varphi_i}{\partial t}=K\sin^2\theta\frac{\partial^2\varphi_i}{\partial x^2}-P_0E\sin\varphi_i+\frac{\Delta\varepsilon\sin^2\theta}{8\pi}E^2\sin2\varphi_i-U[\sin(\varphi_{i-1}-\varphi_i)-\sin(\varphi_i-\varphi_{i+1})]. \quad (2)$$

In the antiferroelectric state the total polarization vanishes when $E=0$. We assume the simplest model for this situation, viz., a herringbone structure in which alternate layers have $\varphi=0$ and $\varphi=\pi$ when the helical structure is suppressed.[18] Those layers with $\varphi=0$ will be unaffected by the applied field, but those with $\varphi=\pi$ will become unstable at sufficiently large fields. We accordingly make the approximation of putting $\varphi_i=0$ for all odd i and $\varphi_i=\varphi$ for even i. Equation (2) then reduces to the single equation

$$\gamma\frac{\partial\varphi}{\partial t}-K\sin^2\theta\frac{\partial^2\varphi}{\partial x^2}=(2U-P_0E)\sin\varphi+\frac{\Delta\varepsilon\sin^2\theta}{8\pi}E^2\sin2\varphi\equiv g(\varphi), \quad (3)$$

where $\varphi\equiv\varphi_2$. An exact solitary-wave solution to Eq. (3) is $\varphi=2\tan^{-1}\{\exp[\sqrt{(-\Delta\varepsilon/\pi K)}(E/2)(x-vt)]\}$.[8–10] For this solution to be physically valid $\Delta\varepsilon$ must be negative.[10] It has been shown to be stable in the limited range of E for which $g'(\varphi)|_{\varphi=0}<0$ when $0<E<E_{th}$ and $g'(\varphi)|_{\varphi=\pi}<0$ when $E>E_{th}$.[8] The velocity v is given by

$$v=\left(P_0-\frac{2U}{E}\right)\frac{2\sqrt{\pi K}}{\gamma\sqrt{-\Delta\varepsilon}}\equiv v_0\frac{E-E_{th}}{E}, \quad (4)$$

with $E_{th}=2U/P_0$ and $v_0=2P_0\sqrt{\pi K}/\gamma\sqrt{-\Delta\varepsilon}$.[19] Physically, this solution corresponds to a region of ferroelecticity (for which $\varphi=0$ in *all* layers) propagating into or retreating from the antiferroelectric region with velocity v.

Taking the literature value $P_0\sim225$ esu cm^{-2},[6] we find that for a typical measured threshold field of $E_{th}\sim250$ statv cm^{-1}, the quantity $2U$ is approximately 5.6×10^4 erg cm^{-3}, or approximately P_0^2; this indicates strong interlayer coupling. We can also examine the velocity profile using Eq. (4). Using a homeotropically aligned and a planar-aligned sample, we measured $\Delta\varepsilon=-1.1\pm0.1$. The velocity data in Fig. 3 is then well described by Eq. (4) if we assume that $\sqrt{K}/\gamma\sim4\times10^{-3}$ cgs. The calculated velocity for these parameters is shown by a solid line in Fig. 3. Since $K\sim10^{-6}$ dyn, our data yields a viscosity $\gamma\sim0.25$ poise, a value typical for liquid crystals. In addition, we note that the experiment was performed at fields close to E_{th}—we were unable to measure the much larger velocities found outside the regime—where v can be approximated by $v_0[(E-E_{th})/E_{th}]$. We find from the model that $v_0\sim3.0$ cm s^{-1}, consistent with the experimental values given in Table I. For $E<E_{th}$ both theory and experiment show that the solitary wave propagates with a negative velocity as the ferrielectric phase is recovered.

If the field is suddenly switched off, we experimentally find that the antiferroelectric phase recovers with a velocity much faster than we can determine with our current apparatus. If the mechanism for this ultrafast recovery of the antiferroelectric phase were solitary-wave propagation, heretofore unobserved in other liquid crystal systems for small fields, then we might expect its velocity to be given by the solution of Eq. (3) with $E=0$. Aronson and Weinberger[12] have rigorously shown this to be $v=v_0\sqrt{-2U\Delta\varepsilon\sin^2\theta/\pi P_0^2}$. To determine the tilt angle θ we observed a planar-aligned sample through a polarizing microscope. The stage of the microscope was rotated to obtain extinction of transmitted light in the presence of large positive and negative dc fields, and θ was found to be $(20\pm1)°$. The velocity v would then be of order 1 cm s^{-1}. Future measurements at higher propagation speeds, fields, and varying temperatures should indicate whether the ferroelectric to antiferroelectric mechanism is front propagation or of some other character, such as bulk relaxation.[10,15]

To summarize, we have experimentally observed a type of reversible solitary-wave-like behavior, with very large ve-

localities, in an antiferroelectric liquid crystal. A simple model was proposed in which a layer-layer coupling was introduced, from which we obtained good agreement with experiment. This system is particularly important, as it provides new insights into nonlinear physics.

This work was supported by the National Science Foundation's Solid state Chemistry program under Grant No. DMR-9502925, and by the Donors of the Petroleum Research Fund, administered by the American Chemical Society.

---

*Present address: Dept. of Physics, MIT, Cambridge, MA 02139.
†Author to whom correspondence should be addressed.

[1] A. D. L. Chandani, T. Hagiwara, Y. Suzuki, Y. Ouchi, H. Takezoe, and A. Fukuda, Jpn. J. Appl. Phys. **27**, L729 (1988).

[2] See A. Fukuda, Y. Takanishi, T. Isozaki, K. Ishikawa, and H. Takezoe, J. Mater. Chem. **4**, 997 (1994).

[3] Y. Yamada, N. Yamamoto, K. Mori, K. Nakamura, T. Hagiwara, Y. Suzuki, I. Kawamura, H. Orighara, and Y. Ishibashi, Jpn. J. Appl. Phys. **29**, 1757 (1990).

[4] R. B. Meyer, L. Liebert, L. Strzelecki, and P. Keller, J. Phys. (Paris) Lett. **36**, L69 (1975).

[5] P. E. Cladis and H. R. Brand, Liq. Cryst. **14**, 1327 (1993).

[6] Y. Suzuki, H. Hagiwara, I. Kawamura, N. Okamura, T. Kitazume, M. Kakimoto, Y. Imai, Y. Ouchi, H. Takezoe, and A. Fukuda, Liq. Cryst. **6**, 167 (1989).

[7] X. Y. Wang and P. L. Taylor (unpublished); in this work the theoretical model is discussed in detail.

[8] E. Magyari, Phys. Rev. B **29**, 7082 (1984).

[9] D. K. Campbell, M. Peyrard, and P. Sodano, Physica **19D**, 204 (1986).

[10] P. E. Cladis and W. van Saarloos, in *Solitons in Liquid Crystals,* edited by L. Lam and J. Prost (Springer-Verlag, New York, 1992).

[11] X. Y. Wang, Phys. Rev. A **32**, 3126 (1985).

[12] D. G. Aronson and H. F. Weinberger, in *Partial Differential Equations and Related Topics*, edited by J. Goldstein (Springer-Verlag, Berlin, 1975); Adv. Math. **30**, 33 (1978).

[13] G. Dee and J. S. Langer, Phys. Rev. Lett. **50**, 383 (1983).

[14] W. van Saarloos, Phys. Rev. A **39**, 6367 (1989).

[15] P. E. Cladis, H. R. Brand, and P. L. Finn, Phys. Rev. A **28**, 512 (1983).

[16] J. E. Maclennan, N. A. Clark, and M. A. Handschy, in *Solitons in Liquid Crystals,* edited by L. Lam and J. Prost (Springer-Verlag, New York, 1992).

[17] W. van Saarloos, M. van Hecke, and R. Holyst, Phys. Rev. E **52**, 1773 (1995).

[18] Y. Galerne and L. Liebert, Phys. Rev. Lett. **66**, 2891 (1991).

[19] Note that $v \lesseqgtr 0$ is determined by the condition $\int_0^\pi g(\varphi) d\varphi \gtreqless 0$.

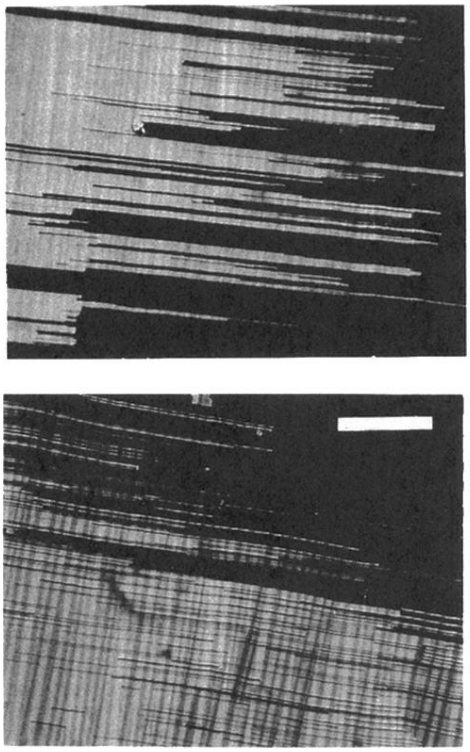

FIG. 2. Polarized photomicrographs of finger textures, both at 110 °C. (a) Nylon treated surface, and (b) polyimide treated surface. The fingering direction corresponds to the $\hat{x}$ axis, and the direction perpendicular to the fingers, but still in the plane of the image, is the $\hat{z}$ axis. The fingers were stabilized at an electric field just above E_{th}, and the polarizer and analyzer were oriented along the $\hat{y}$ and $\hat{z}$ axes, respectively (see Fig. 1). A 100-μm-long bar is shown in the lower figure.